Motion Analysis of Rainy Cells Observed In Weather Radar Images

O. Raaf *, A. Adane*

** Faculty of Electronics and Computer Science,*
University of Science and Technology Houari Boumediene (U.S.T.H.B.),
Po box 32 El Alia, Bab Ezzouar 16111, Algiers, Algeria.
(Tel: +213 2124 79 50; e-mail: rf_ouarda@ yahoo.fr).

Abstract: This paper concerns the estimation of rainy cells motion observed in meteorological radar images using optical flow method. To characterize and predict the evolution of rainy clouds in real-time, series of PPI filtered images were collected at the meteorological station of Setif (Algeria). These images of 512x512 pixels were collected every 5 minutes by non-coherent radar working at 5.6 GHz. After filtering echoes of ground present in radar images, we applied the method of 'Lucas-Kanade' and another method based on Gabor filters. In both cases the estimated optical flow shows all the moving cells in the considered image sequences.

Keywords**:** Differential Method, Motion estimation, Optical flow, Radar images, Rainy cloud.

1. INTRODUCTION

Since several years, the forecasting of rain in the short time limit was a topic of meteorologist interest. A network of rain gauges gives the punctual and direct measures of rain rate on the ground that it is possible to interpolate in order to reconstitute the complete rainy field. This operation is not very reliable when rain presents a large spatial variability. In this case, meteorological radars are the only instruments which can finely describe the development of the rainy field in a radius of several kilometres. The radar equipment represents rain cells with: position, shape, intensity, dimensions and displacement (Meischner, 2005, Sauvageot, 1992). The radar data can be used to detect other sever atmospheric phenomena's such as hail storms and tornados. It is therefore necessary to identify and follow rainstorms in order to define their trajectories and intensities. The use of meteorological radars is delicate because of the earth relief which produces masque effects and degrades noticeably rain echoes detection and reduces radar performance. It is therefore essential to remove this clutter to be able to follow the evolution of the precipitation echoes (Darricau, 1993).

The motion estimation from an image sequence is used in several applications. In robotics, it can identify and anticipate changes in the position of objects. In video compression, it allows the fullest possible understanding where the temporal redundancy of the sequence and information describing an image using the surrounding images. In meteorology it allows the detection and forecasting of rainy cloud including those which are dangerous and predicting their motion(Fabry and *al*., 2009).

The movement, in a sequence of images is visible through changes in spatial distribution of a variable photometric between two successive images, such as luminance, brightness, or reflectivity which is the variable used in meteorological images. The use of non-linear algorithms became necessary, which opened the signal processing and modern mathematics to the study of such a random phenomenon. In this context, we are interesting in this paper to the detection and extraction of the velocity of rainfall from radar images using optical flow. Specifically, we will treat the part 'low level' which provides local information on the speed as a field of velocity. Given these objectives, we introduce the database used in this study then we will formulate the optical flow equation used to calculate the velocity fields in artificial images and weather radar images(Bruno,2001; Neill and *al.*, 2004).

2. DATA BANK

The studied images in this paper were collected with meteorological radar ASWR 81(Algerian Service Weather Radar) installed in the city of Maghras in Setif (36 °11N, 05°25E, altitude 1730 m) in the north-east of Algeria where they are known as high plateaus. In figure 1, we present an example of radar image taken in December 26th, 2004 at 17:30 where the radar is in the middle of the picture. In this figure, the fixed echoes reflected from mountains appear.

Indeed, at the west of Setif we can discern an orange band due to the presence of regional mountain ranges known as Djurdjura where the highest elevation corresponds to Lalla Khadidja Mountain (2308 m). At the south and at the north of the radar we can observe a bluish zone corresponding respectively to Bibans and Babor ranges. The border limits are represented in red. The resolution of this image is 1Km par pixel in PPI (Plan Position Indicator) representation**.** Its format is 512×512 pixels with 16 reflectivity levels. Also on this figure, we can see rain echoes represented as a quasi-homogeneous structure whereas the fixed echoes are scattered in small cells of non homogeneous intensity. The suppression of mountainous echoes that constitute a parasitic signal in the forecasting and the quantification of rain cells is made by using a masque method combined to a shape detection. This method consists to subtracting in the study image the mask constructed from images in clear sky, and then remove the residual cell occupies a small area (Raaf and *al.*, 2008).

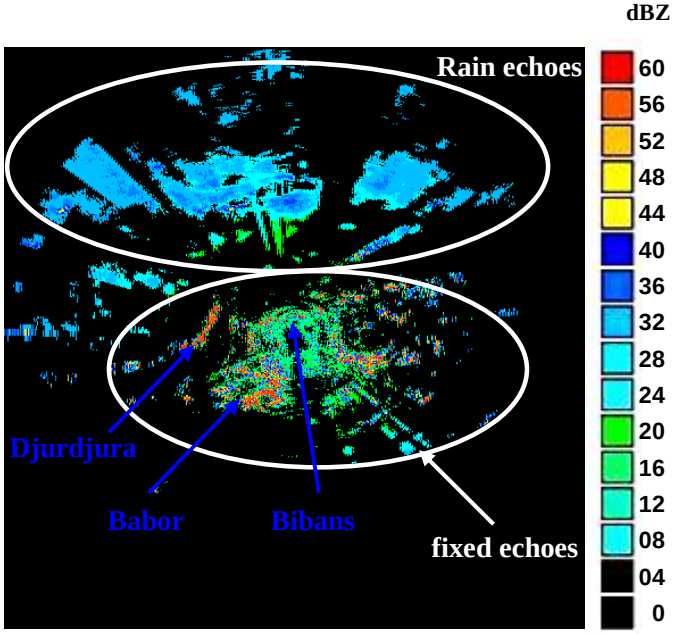

Fig. 1. Radar image of the region of Setif.

3. MOTION ESTIMATION USING OPTICAL FLOW

3.1 Optical flow equation

The motion estimation is based on that a point has instituted a fixed image. It can therefore be matched between two consecutive images estimate the motion of the point by the method of optical flow (Baron and Al., 1994; Ménin, 2003). A sequence of images can be represented by its brightness function *I (x, y, t).* The hypothesis of conservation of brightness provides that a physical point of the image sequence does not vary with time, which gives:

$$I(p,t) = I\ (p\ + V(p)\,\delta t, t+\delta t) \qquad (1)$$

p (x, y) is one point of the image and *V (p) = V (u, v)* is velocity vector at point *p* at time *t*. The components *u* and *v* are respectively the velocity along *x* and *y.*

Equation (1) lead to the annulment of the inter-image difference moved. Assuming that *I (x, y, t)* is a continuous function and its time derivative, the assumption of conservation of the luminance is written by:

$$\frac{dI}{dt} = \frac{\delta I}{\delta t} + \nabla I.V = 0 \qquad (2)$$

Where: $\nabla I = \left[\frac{\delta I}{\delta x}, \frac{\delta I}{\delta y}\right]$ is the spatial gradient of *I.*

Several models have been used to solve the equation of optical flow as the model of translation, the parametric model and the nonparametric model. In this study we are interested in determining the velocity field seen in a sequence of radar images using the nonparametric differential methods.

3.2 Differential Method

The differential methods belong to the techniques commonly used for the calculation of optical flow in image sequences. Their advantages are reductions in the complexity of calculations commonly used in the matching methods while increasing the range of measurable displacements. They can be classified in two: Global methods such as the technique of Horn and Schunck and Local as the Lucas-Kanade approach and that based on Gabor filters. These methods are based on the equation of the apparent motion (ECMA) issue to Taylor development of the equation of the intensity *I (x, y, t)* given by(Bainbridge-Smith and *al.*, 1997):

$$I(x+dx, y+dy, t+dt) = I(x,y,t) + \frac{\delta I}{\delta x}dx + \frac{\delta I}{\delta y}dy + \frac{\delta I}{\delta t}dt + o(\varepsilon) \qquad (3)$$

Where ε gives terms of higher order of Taylor development of first order and tends to 0 when *dt* tends to *0*.

So we get:

$$uI_x + vI_y + I_t = 0 \qquad (4)$$

I_x, I_y , I_t: spatio-temporal derivative of intensity at point *p (x, y)* at time *t.*

To solve this equation by respecting the conditions of validity two solutions are proposed in this study: the Lucas-Kanade method and Gabor filters.

Lucas and Kanade method :

The method proposed by Lucas and Kanade is a local approach. It is based on the supposition that the motion is uniform over a region of the image or that the optical flow is

constant over Ω neighbourhood centred on the pixel that we want to calculate the displacement. We are therefore leading to minimize the following functional(Bouguet, 2000):

$$E = \sum_{\Omega} [\nabla I.V(p_i) + I_t]^2 \quad (5)$$

Ω is a window around the point at which you wish to determine the scope of the movement.

In this method each calculation is done on a small window in parallel independently of other windows. The solution is to make an estimate in the sense of least square. In matrix notation the solution is:

$$V = (A^T A)^{-1} A^T b \quad (6)$$

$$\text{With : } A = \begin{bmatrix} I_{x1} & I_{y1} \\ I_{x2} & I_{y2} \\ I_{xn} & I_{xy} \end{bmatrix}, b = \begin{bmatrix} I_{t1} \\ I_{t2} \\ I_{tn} \end{bmatrix}$$

It may happen that the matrix A^TA is ill conditioned (almost zero determinant and therefore not invertible). This is because the pixel is in an area where the luminance intensity is constant on an area where a zero gradient (Problem opening) and the estimate in the sense of least squares of *V* becomes aberrant. We can remedy these problems by using a regularization technique. We can then write:

$$E = \sum_{\Omega} [\nabla I.V(p_i) + I_t]^2 + \alpha V^2 \quad (7)$$

With α (adjustable) representing the regularity of the solution. This equation is always linear and can yield to the following:

$$V = (A^T A + \alpha J)^{-1} A^T b \quad (8)$$

J: identity matrix

The optic flow equation that we developed is valid only if the displacement is small, so we have to use the multi-resolution, which was developed in the algorithm of Horn and Schunck. On the other hand, it is possible to further refine the results at each level of the pyramid minimizing the gap between two successive frames and running again the algorithm after moving one of two images according to the latest calculated field velocity. If the algorithm is stable, the method converges and therefore:

$$V^l = V^{l-1} + \eta^l \quad (9)$$

with $V^0 = 0$ et $\eta^1 = (A^T A + \alpha J)^{-1} A^T b_l$

If *L* iterations are necessary to achieve convergence, therefore the final solution is the last calculated vector given by:

$$V = \sum_{l=1}^{L} V^l \quad (10)$$

Method based on Gabor filters

Gabor filters are widely used in computer vision. This success is due both to their spatial and spectral properties. E. Bruno has proposed a novel approach with is drawn on the differential method for local estimation of optical flow from Gabor filter banks [10]. It is based on projection the optical flow equation (4) into a pixel image on a bank of N Gabor filters. We obtain an over determined system of *N* equations that allows us to calculate the two velocity components of the pixel considered.

Assuming that *V* is constant over the filter support G_k we can write the optical flow equation as (Bruno, 2001):

$$u(\frac{\delta I}{\delta x} * G_i) + v(\frac{\delta I}{\delta y} * G_i) + \frac{\delta I}{\delta t} * G_i = 0 \quad i=1\ldots N \quad (11)$$

The minimization is obtained iteratively by the least squares algorithm weighted iterated (MCPI):

$$V = \arg\min \sum_i w_i \rho(r_i) \quad (12)$$

With $w(x) = \frac{1}{x}\frac{\delta \rho(x)}{\delta x}$ is a weighting function and ρ (x) is a Euclidean norm.

The choice of the function *ρ (x)* can be done in a wide range of functions. It must be even defined, positive and should not have a single minimum at zero. In addition, for the function ρ (x) minimizes the influence of bad data, it must be less than the quadratic function. In the case of a local estimate, it is preferable that the aberrant data be deleted. So we chose to use the M-estimator (Huber, 1981)

4. APPLICATION

The Lucas and Kanade and Gabor algorithm were tested on 3 different sequence images: a cube, taxi and a rainy cell (Figures 2.a, 3.a, 4.a and 4.b).

• The Artificial Sequence 'cube' consisting of a cube placed on a turntable plateau, the image size is 256 × 240 pixels.

• The Artificial Sequence 'taxi' is a street intersection. It is composed of three cars and a pedestrian moving. The two bottom vehicles moving in opposite directions. The taxi turned the corner in the middle of the street; the image size is 256 × 190 pixels.

• The sequence of two stratiform cells isolated from images of size 64 × 64 pixels taken in December 26th, 2004 at 17:30(Figure 4.a) and fifteen minute after (Figure4.b). The first cell has 2685 km^2 of surface and 19.44 dBZ of reflectivity.

5. RESULTS AND INTERPRETATIONS

5.1 Lucas and Kanade method

The gradient that gave the best results was calculated using the mask [-1 1, -1 1] for a horizontal displacement *x*, and [-1 -1, 1 1] for vertical *y*. After several trial tests, the best results were obtained under the following conditions:

- The cube level of the pyramid 3, patch 7 × 7 pixels, alpha = 10^{-3}: the velocity field in figure 2.b shown the rotation of the plateau.
- Taxi: level of the pyramid 3, patch 7 × 7 pixels, alpha = 10^{-3}: Figure 3.b shows three cars moving that both are gray moving in opposite directions and white taxi in the center that turns on the corner. The movement of the pedestrian is not detected.
- Rainy cell: pyramid level 1 patch of 5 × 5 pixels, alpha = 10^{-3} : in Figure 4.c appears vectors almost directed to the right indicating the direction of development of rainy clod. We also note that the estimated motion is almost zero at the center of the cell and increases gradually as we come near the edges, which is logical because the cloud changes little in 15min and. Outside the rain cell the field is considered zero. Also, the size of images used in the sequences Cube and taxi is important is that justifies the use of third-level pyramid. Concerning the cell extracted rain weather radar images we used the first level directly given the size of the image.

5.2 Gabor Filter method

We find that the estimated flow shows all the objects in motion in the three sequences of images. The tuning parameters of this algorithm do not differ greatly in all three cases, thus:

- Cube (fig. 2.c): K=3, alpha=10^{-3}, σ=4, f_0=0.14 .
- Taxi(fig. 3.c): K=3, alpha=10^{-3}, σ=4, f_0=0.18 .
- Rain cell (fig.4.d): K=1, alpha=10^{-3}, σ=4, f_0=0.14.

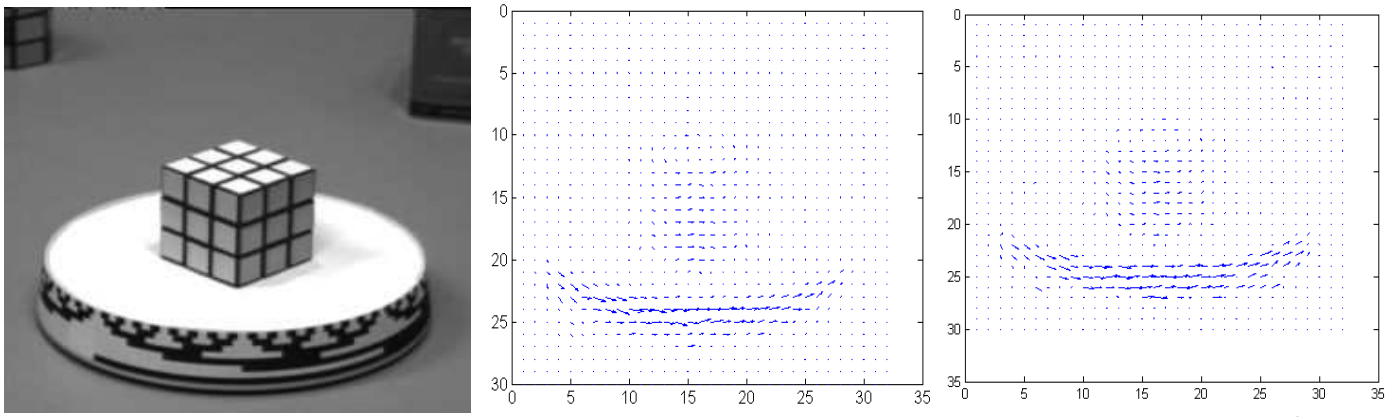

(a) : Cube Image (b): Field estimated by Lucas-Kanade (c): Field estimated by Gabor filters

Fig. 2 : Optical flow estimated for Cube Image by patch 7×7

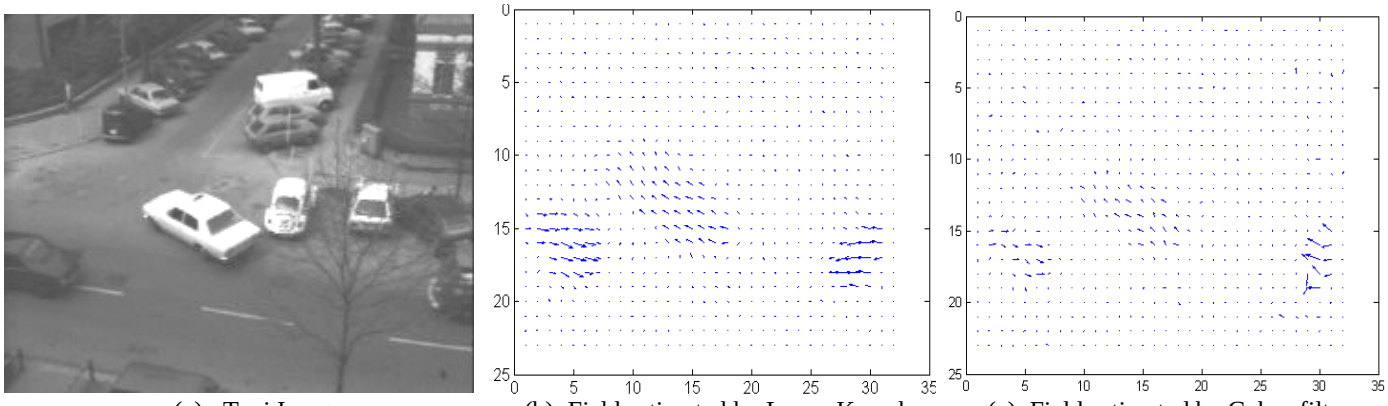

(a) : Taxi Image (b) :Field estimated by Lucas-Kanade (c): Field estimated by Gabor filters

Fig. 3 : Optical flow estimated for Taxi Image by patch 7×7.

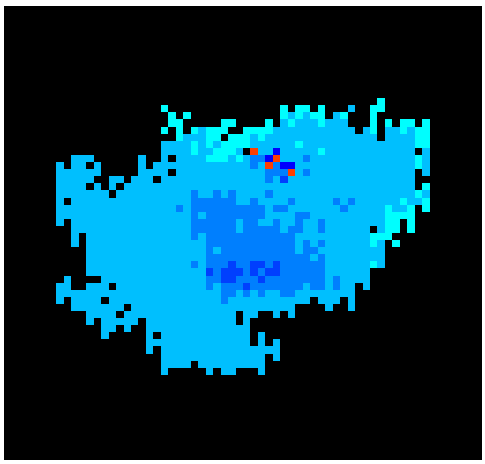

(a): 1st Cell of rainy cloud

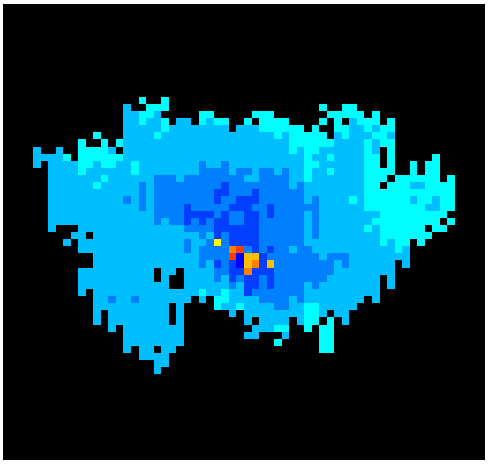

(b): 2nd Cell of rainy cloud

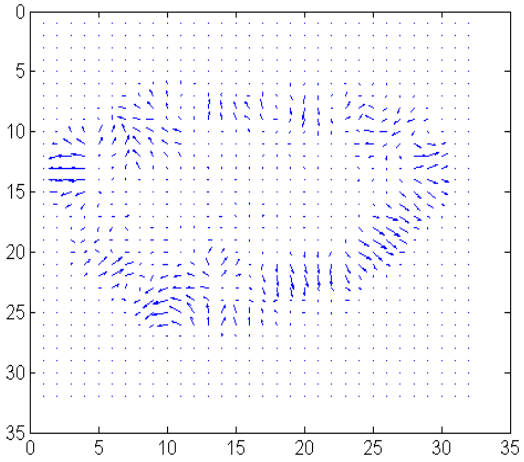

(c): Field estimated by Lucas-Kanade method

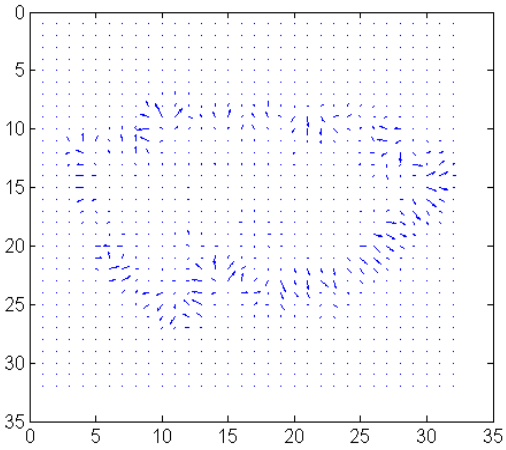

(d) Field estimated by Gabor filters

Fig. 4 : Optical flow estimated for rainy cell

We also note that the density increases with velocity vectors N to reach a step where it does not change, for N = 6. However, the increment of N greatly increases the computing time. The density also increases with σ up to a maximum value beyond which we obtain a smooth velocity field, since the assumption of locally constant optical flow is no longer respected. We also note that variations of the frequency centre are very low this is due to that the global variations of the considered photometric variable (brightness or reflectivity) are low-frequency type.

On setting the parameters for obtaining good results, there is a trade-off between alpha and the number of iterations since the higher the number of iterations is large there are more better movement area boundaries

In these three examples we have considered a single iteration loop for refinement: i,e: $L = 1$. Increasing L will have little influence on the velocity fields of moving objects. Tests on the size of the patch showed that whenever the window size is increase, an optic flow appears which is more and more dense until reaching an optimum value. Thus, if we continue to increase the window size, the optic flow becomes smooth, ie the contour areas will begin to disappear and the movement becomes less clear.

6. CONCLUSIONS

In this paper we have presented two techniques for estimating local motion of rainy cells in which the quality of estimation depends mainly on the right choice of the parameters in each method. In both cases the estimated optical flow shows all the objects moving in three sequences of images. We also found that the method based on Gabor filters gives a less dense optical

flow with a lack of precision in the estimated field near the border. This was in contrast with the method of Lucas and Kanade. Moreover, it was found that the computing time required to run the algorithm of the latter is much smaller than that of the Gabor filters.

REFERENCES

Baron JL., Fleet DJ. and Beauchemin SS.(1994). Performance of optical flow techniques. *In International Journal on Computer Vision*, vol. 12, pp. 43-77.

Bainbridge-Smith, A. and Lane, R. G., Determining optical flow using a differential method Image and Vision Computing, Volume 15, Issue 1, January 1997, Pages 11-22.

Bouguet J.(2000). Pyramidal Implementation of the Lucas Kanade Feature tracker, Intel Corporation, Microprocessor Research Labs .

Bruno E (2001). De l'estimation locale à l'estimation globale de mouvement dans les séquences d'images. Thèse, Université Joseph Fourier, Grenoble, France.

Darricau, Y.(1993), Physique et théorie du radar, Tome I et II, Sodye (Ed), Paris.

Fabry, F. and Seed, A. W. , Quantifying and predicting the accuracy of radar-based quantitative precipitation forecasts, Advances in Water Resources, Volume 32, Issue 7, July 2009, Pages 1043-1049.

Huber P.(1981). Robust statistics, Wiley(Ed), New York.

Meischner, A.(2005). Weather radar: principles and advanced applications. Springer.

Mémin E; Juillet 2003. Estimation du flot optique-contribution et panorama des différents approches ; Habilitation à diriger des recherches. Université de Rennes 1,Rennes.

Neill E. H. Bowler, Clive E. Pierce, Alan Seed, Development of a precipitation nowcasting algorithm based upon optical flow techniques, Journal of Hydrology, Volume 288, Issues 1-2, 20 March 2004, Pages 74-91

Raaf, O. and Adane, A.(2008). Image-Filtering Techniques for meteorological radar. *In International Symposium on Industrial Electronics* (IEEE ISIE08), 30 June-02 July 2008, Cambridge, pp. 2561-2565.

Sauvageot , H.(1992). Radar Meteorology. Artech House(Ed), Boston.